Electronic Supplementary Material (ESI) for Energy Advances.

Supporting Information: Lithium Dynamics at Grain Boundaries of β-Li_3PS_4 Solid Electrolyte

Randy Jalem,[†,‡] Manas Likhit Holekevi Chandrappa,[†] Ji Qi,[†] Yoshitaka Tateyama,[‡] and Shyue Ping Ong[*,†]

†*Department of NanoEngineering, University of California San Diego, 9500 Gilman Dr, Mail Code 0448, La Jolla, CA 92093-0448, United States*

‡*Center for Green Research on Energy and Environmental Materials, National Institute for Materials Science (NIMS), Tsukuba, Japan*

E-mail: ongsp@eng.ucsd.edu

GB structure generation

The GB structure set for MTP fitting was constructed based on the coincidence site lattice (CSL) method,[S1] it comprised with 15 stoichiometric GB models in the Σ3 and Σ5 boundaries. Higher Σ boundaries (e.g., Σ13, Σ25) and GB structures with amorphous-crystal contact were also generated and used for the subsequent large-scale MD study. Additional details for GB structure construction of the amorphous-crystal GB structures are provided (Table S1 and Figure S2, respectively). The GB structures used in the actual MD production runs were derived from lowest-energy structures of a geometry relaxation procedure on ion coordinates and cell volume. In addition, the lateral shift of the GB interface was also optimized by grid search method within a 4 Å x 4 Å grid area and at a grid size of 1 Å. Figure S1 shows two representative GB models, Σ5[001]/(120) tilt GB (tilt angle $\alpha_1 = 53.13°$) and Σ5[001]/(001) twist GB (twist angle $\alpha_2 = 180°$) with 10,240 and 12,800 atoms, respectively. The *GB energy* of a GB structure was calculated using the following equation:

$$GB\ energy = (E_{GB} - NE_{bulk})/2A, \tag{1}$$

where E_{GB} is the total energy of the GB model structure, E_{bulk} is the total energy of the bulk structure, N is the number of units of the bulk to match the GB stoichiometry, and A is the slab cross-sectional area.

Construction of GB seed structures of β-LPS for MTP training

Table S1 shows the structural information of seed GB structures (tilt and twist GBs) that were used for the active learning procedure of the MTP development. The rotation axis and the crystal plane direction were set to a maximal Miller index of 1 and 2, respectively, to keep the system size (<400 atoms) computationally manageable for DFT single-point calculations which in turn generate the train and test datasets of total energies and ion forces.

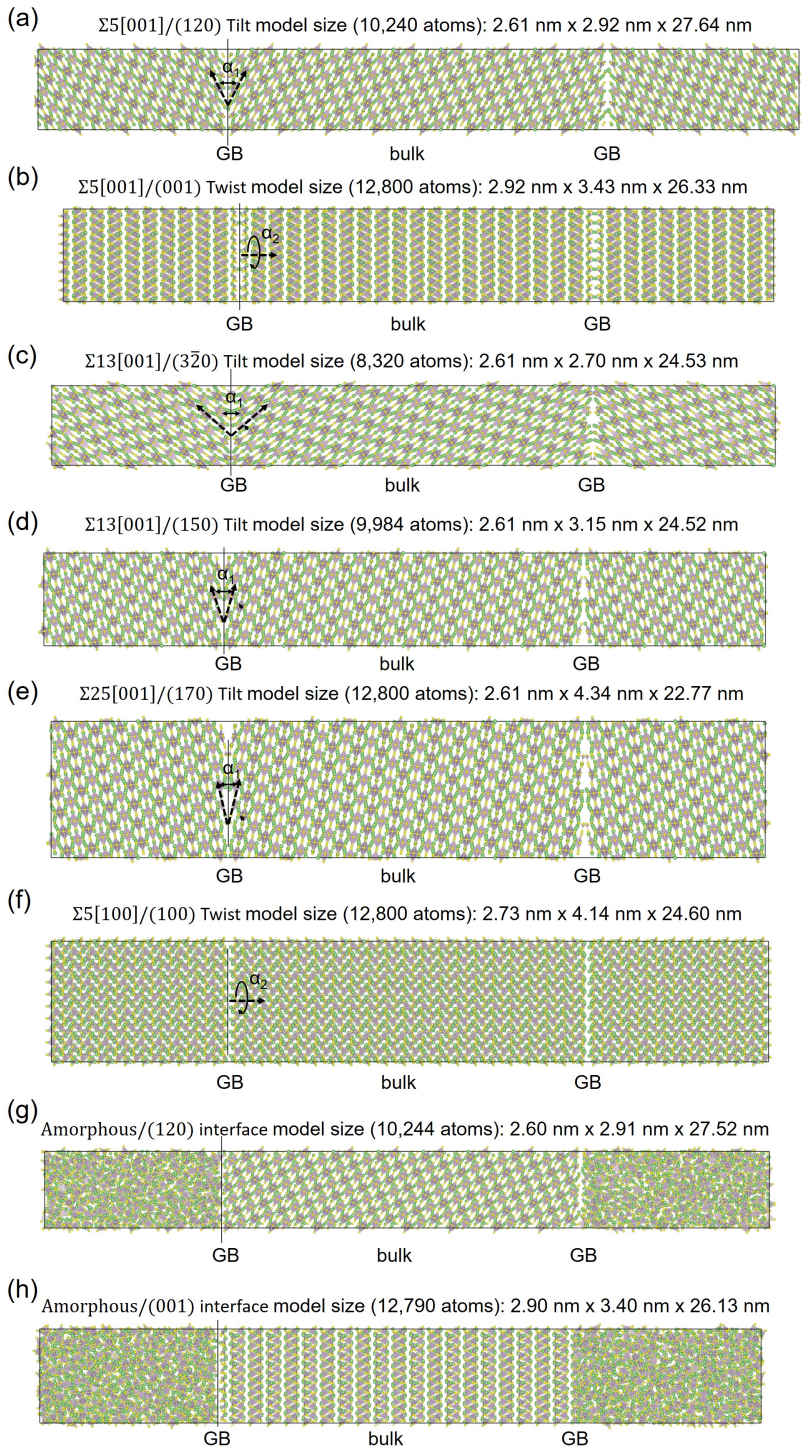

Figure S1: Representative GB structure models constructed under periodic boundary condition: (a) Σ5[001]/(120) tilt GB (tilt angle $\alpha_1 = 53.13°$), (b) Σ5[001]/(001) twist GB (twist angle $\alpha_2 = 180°$), (c) Σ13[001]/(3-20) tilt GB (tilt angle $\alpha_1 = 67.38°$), (d) Σ13[001]/(150) tilt GB (tilt angle $\alpha_1 = 22.62°$), (e) Σ25[001]/(170) tilt GB (tilt angle $\alpha_1 = 16.26°$), (f) Σ5[100]/(100) twist GB, (g) Amorphous/(120) interface, and (h) Amorphous/(001) interface. PS_4 unit and Li atom are shown as tetrahedron and green spheres, respectively.

Table S1: Structural lattice information of generated DFT-relaxed GB structures from bulk β-LPS.

GB structure	Cell edge a (Å)	Cell edge b (Å)	Cell edge c (Å)	#atoms
Σ5[001]/(120) tilt	14.5989	34.3035	13.0660	320
Σ5[001]/(2-10) tilt	29.1979	17.1518	13.0660	320
Σ5[010]/(10-2) tilt	17.8776	53.6695	8.0150	320
Σ5[010]/(201) tilt	35.7552	26.8347	8.0150	320
Σ5[100]/(0-21) tilt	27.3335	41.3609	6.1010	320
Σ5[100]/(012) tilt	54.6670	20.6805	6.1010	320
Σ3[110]/(1-12) tilt	16.4980	56.0123	10.0729	384
Σ3[110]/(111) tilt	32.9959	28.0061	10.0729	384
Σ3[111]/(1-21) tilt	43.1232	14.4202	16.4980	384
Σ3[111]/(10-1) tilt	21.5616	28.8404	16.4980	384
Σ5[001]/(001) twist	14.5989	17.1518	26.1320	320
Σ5[010]/(010) twist	17.8776	26.8347	16.0300	320
Σ5[100]/(100) twist	27.3335	20.6805	12.2020	320
Σ3[110]/(110) twist	16.4980	28.0061	20.1457	384
Σ3[111]/(111) twist	21.5616	14.4202	32.9959	384

Construction of amorphous-crystal GB structures of β-LPS for use in MD runs with trained moment tensor potential

Figure S2 shows the schematic illustration for the procedure of constructing crystal-amorphous interface structure. Initially, a portion of the MD-generated amorphous structure in the longest-axis direction was cut out and removed. Separately, a crystal slab structure terminated at both ends by the targeted GB plane (e.g., (120)) was inserted into the cut-out open region of the amorphized structure, resulting into a crystal-amorphous interface structure.

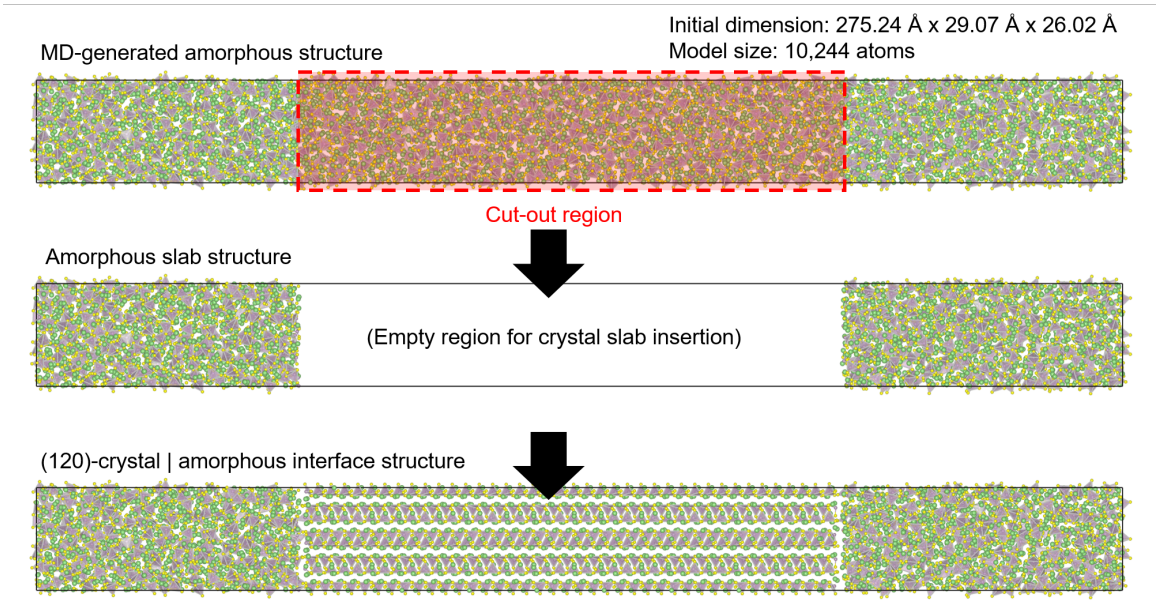

Figure S2: Construction procedure of the amorphous/(120) GB structure model.

Formation of topological ring structure by persistent homology

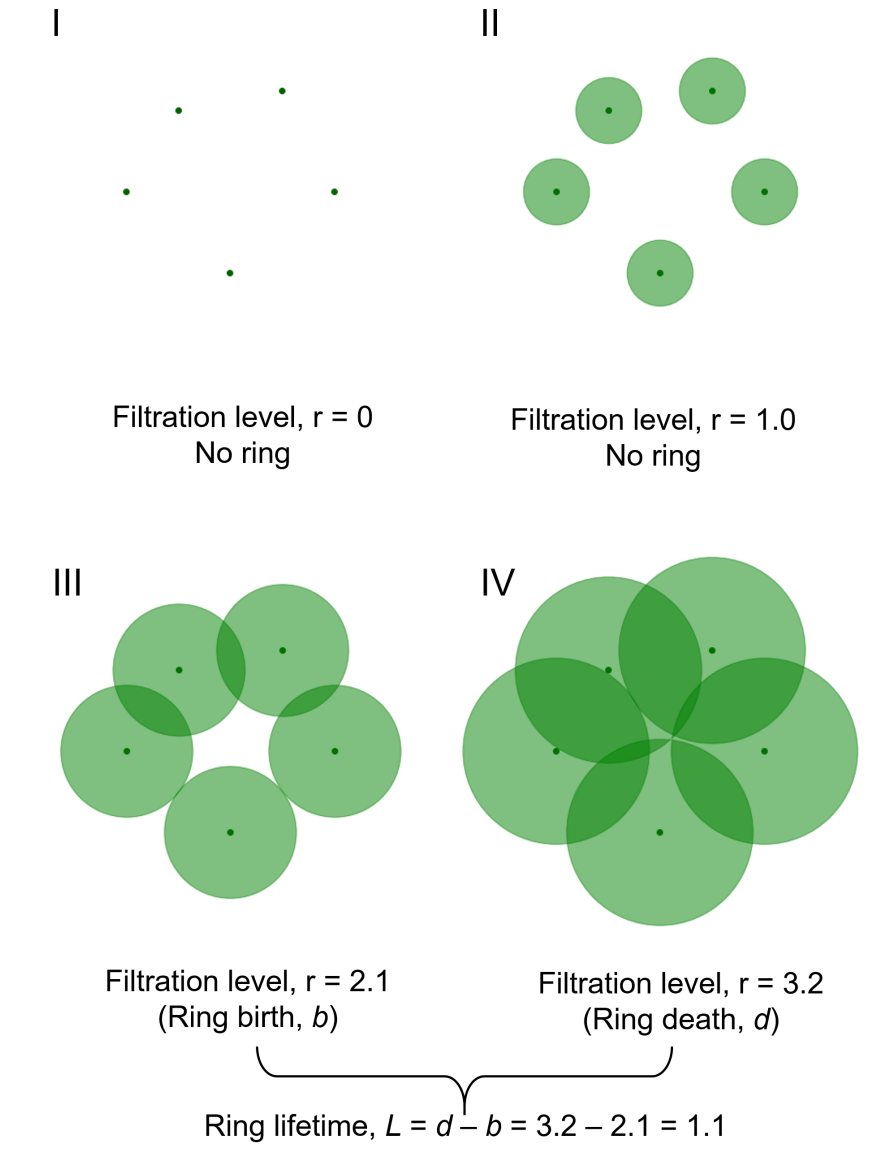

Figure S3: A schematic picture showing the sequence of increasing sphere radii related to a set of points, starting from a size of zero up to ring birth (b) and ring death (d). Ring lifetime (L) is calculated from the difference between d and b.

MTP hyperparameter tuning details

Figure S4 shows MTP hyperparameter tuning results from passive learning using bulk β-LPS structures (calculated by optB88-vdW functional). Two parameters, MTP basis number (n_{basis}) and cutoff radius (r_{cut}), were optimized; the MAE values for energies and ion forces were used as validation metrics. Of the hyperparameter values that were tested (i.e., n_{basis} = [8, 10, 12, 14, 16, 18, 20], r_{cut} = [4.0, 5.0, 6.0, 7.0] Å), the corresponding MAE values for energies and ion forces (see Figure S4a, S4b are shown to be low and in a narrow range (i.e., 3.2 - 7.1 meV/atom and 0.095 - 0.172 eV/Å, respectively). Given the minimal differences in MAE values, the MTP model complexity (i.e., number of degrees of freedom) is also considered as another criterion to select a reasonable combination of n_{basis} and r_{cut}. The number of degrees of freedom of MTP (N_{DOF}) is calculated according to the following equation:

$$N_{DOF} = n + b_s \times f_c \times n^2 + m_\alpha \tag{2}$$

where n is the number of elements in the Li-P-S system, b_s is the radial basis size, f_c is the radial function count, and m_α is the alpha scalar moments. Figure S4c shows the polynomial increase of N_{DOF} with respect to n_{basis} for the Li-P-S system. Based on the combined results on MAE values and the number of degrees of freedom, a combination of r_{cut} = 5.0 Å and n_{basis} = 14 was chosen as the hyperparameter combination to be employed for the MTP active learning phase.

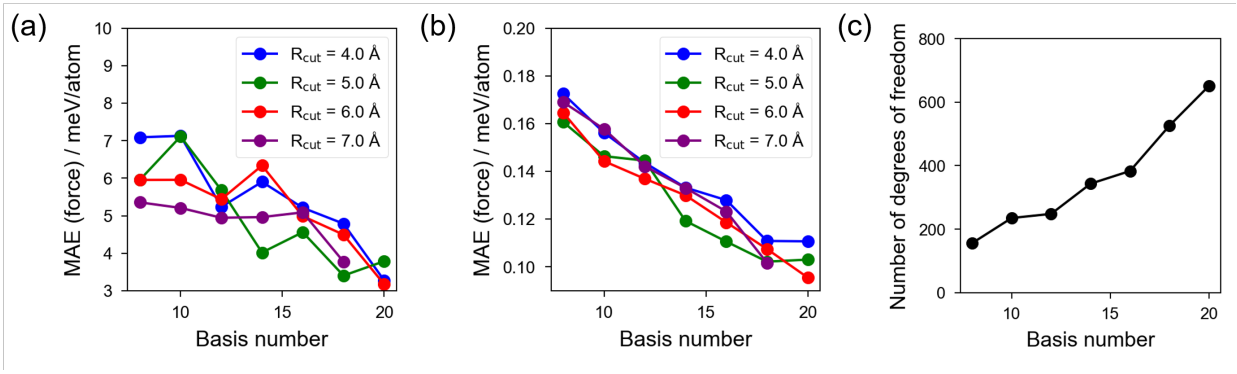

Figure S4: MTP hyperparameter tuning results from passive learning using bulk β-LPS structures (270/30 training/test structures): MAE in (a) energies and (b) ion forces as a function of n_{basis}, respectively. (c) Plot of the MTP complexity (i.e., N_{DOF}) as a function of n_{basis}.

MTP active learning results

Figure S5 displays the number of selected GB structures that were added to the training set at every active-learning step. The maximum number of selected structures is 77 which is at the 11^{th} step. Overall, a total of 599 selected GB structures was collected into the training set after 17 steps, with the last step having no structures being selected based on the extrapolation grade parameter γ_{break}. The 17^{th} step was then regarded as the termination point of the active learning task.

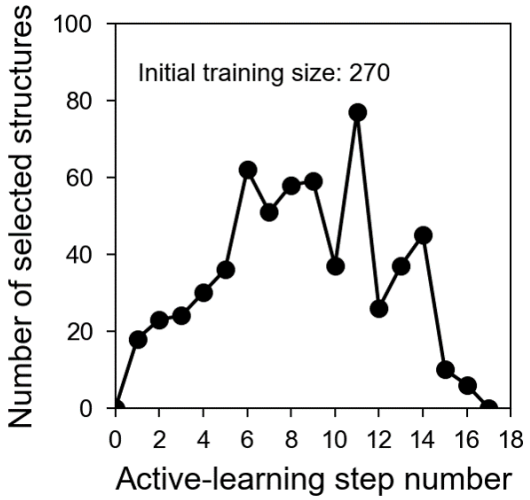

Figure S5: Plot of number of selected GB structures (to add to the training set) as a function of active-learning step number. The initial training set contains 270 β-LPS bulk structures generated by AIMD at different temperatures (300-2000 K).

MAEs in energies and ion forces for bulk crystal and amorphous LPS by trained MTP

Figure S6 shows the fitting quality results for energies and ion forces between DFT-optB88 and MTP single-point calculations for the bulk crystal and amorphous LPS. The overall test-MAE values are shown to be reasonably low: 11.9 meV/atom and 114.7 meV/ Å, respectively.

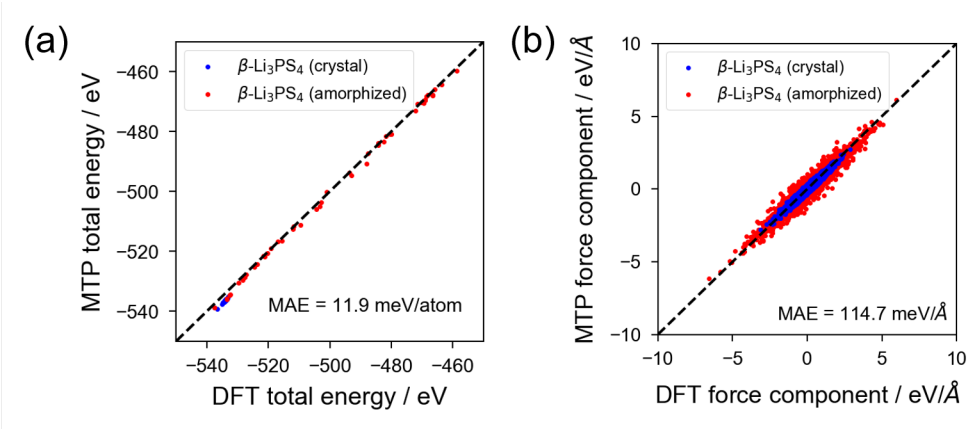

Figure S6: Fitting quality of the trained moment tensor potential (MTP) vs. DFT-optB88 test dataset for bulk crystal and amorphous LPS structures: (a) energies and (b) ion forces.

Element-based MSD plots of GB and interface models

Figure S7 shows the element-based MSD plots for different GB and interface models from 300-K MTP-MD runs. The Li ions are determined to be the main diffusing species (i.e., positive MSD slope) while non-Li ions are found to only vibrate about their positions (i.e., flat MSD slope).

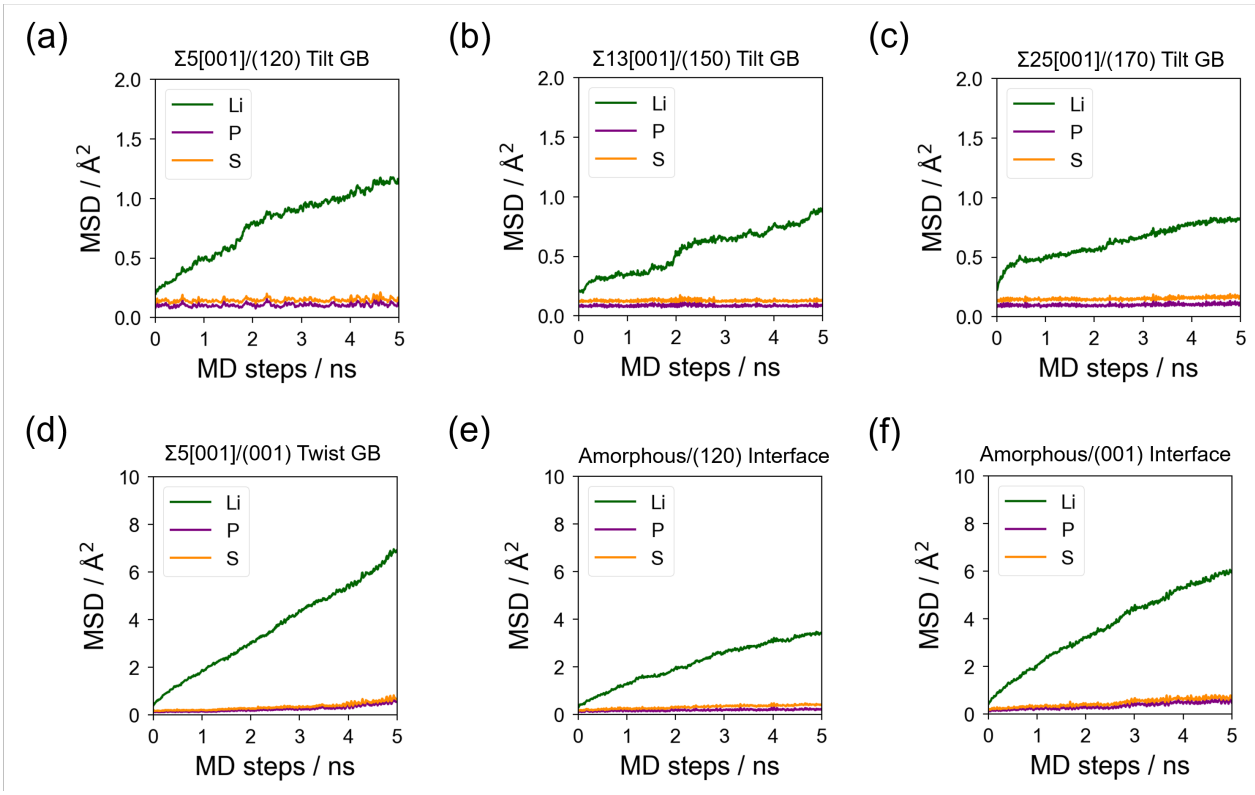

Figure S7: Element-based MSD plots of different GB and interface structures of β-LPS from 300-K MTP-MD trajectories: (a) Σ5[001]/(120) tilt GB, (b) Σ13[001]/(150) tilt GB, (c) Σ25[001]/(170) tilt GB, (d) Σ5[001]/(001) twist GB, (e) amorphous/(120) interface, and (f) amorphous/(001) interface.

MD-derived P and S heatmap at 300 K in GB and interface models

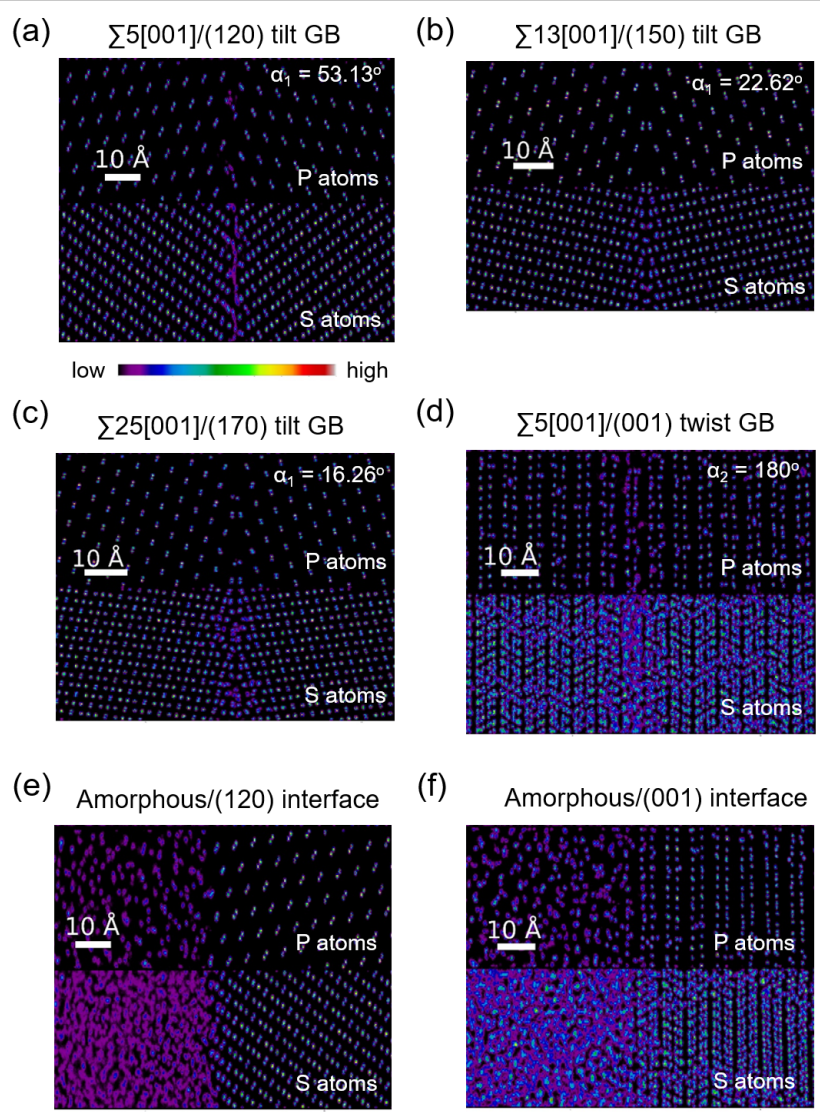

Figure S8: 2D-projected atom-count heatmaps for P and S atoms from different GB structures as derived from NPT-MD calculations at 300 K: (a) Σ5[001]/(120) tilt GB, (b) Σ13[001]/(150) tilt GB, (c) Σ25[001]/(170) tilt GB, (d) Σ5[001]/(001) twist GB, (e) amorphous/(120) GB, and (f) amorphous/(001) GB. The length scale in the images is shown by horizontal white line (10 Å).

Diffusion behaviors at dislocation cores of GB structures

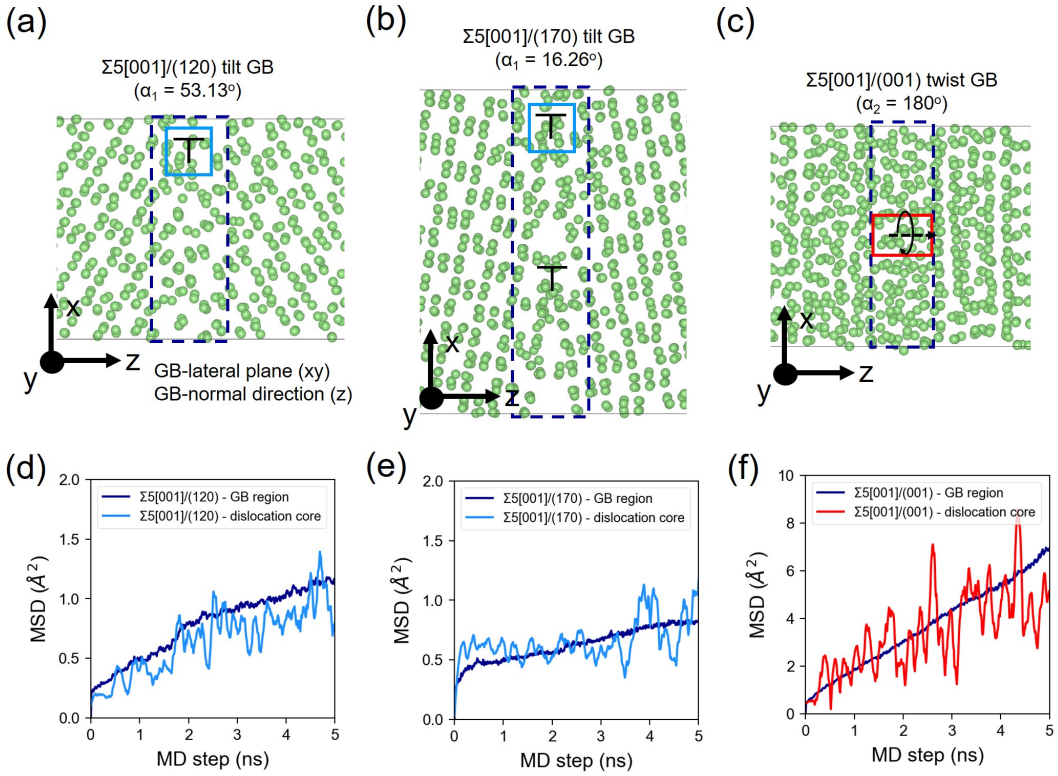

Figure S9: Schematic pictures showing the dislocation cores in the GB region of (a) Σ5[001]/(120) tilt GB ($\alpha_1 = 53.13°$), (b) Σ5[001]/(170) tilt GB ($\alpha_1 = 16.26°$) and (c) Σ5[001]/(001) twist GB ($\alpha_2 = 180°$), as viewed using the Li sublattice. The GB structures were taken from one of the 300-K MD trajectory snapshots. The corresponding Li MSD plots for the GB and the dislocation core regions are displayed in (d), (e), and (f), respectively. Dislocation-core MSD sampling was performed within the small (3D) solid box (light blue for tilt GB, red for twist GB), while the GB-region MSD sampling was performed within the larger (3D) dashed-line box (dark blue). For the tilt GB, the dislocation core region was assigned with a dimension of 5 Å x b x 5 Å, where b is the GB cell length in the y-direction. For the twist GB, the dislocation core was assigned with a dimension of 5 Å x 5 Å x 10 Å, with the core center located along the twist rotation axis.

Visualization of Li ring sub-networks in GB structures

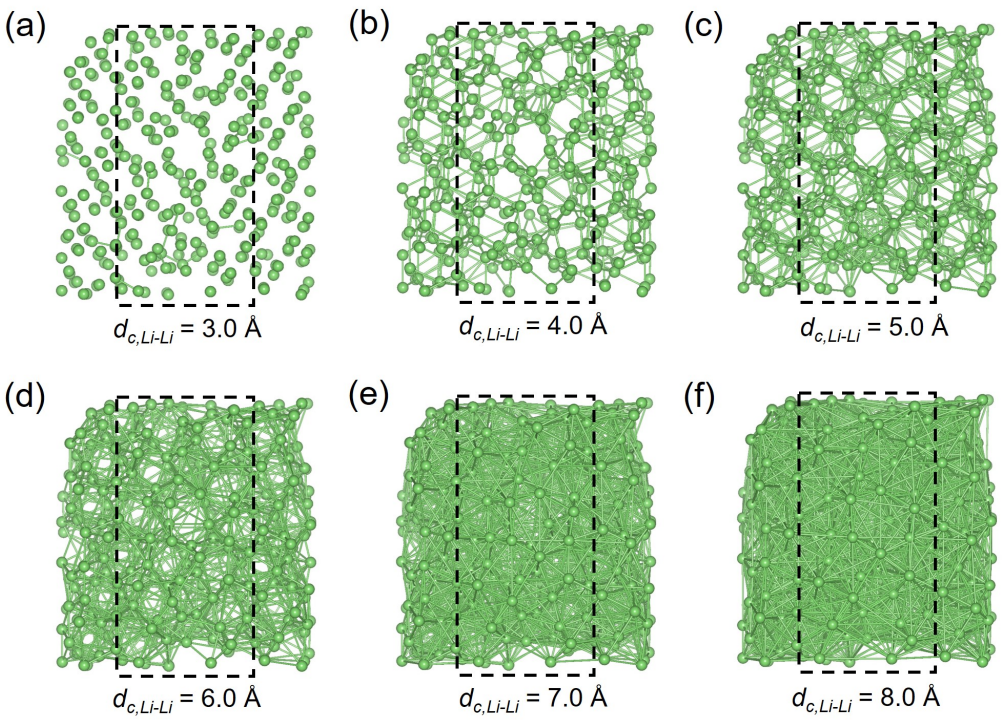

Figure S10: (a-f) Visualization of the formation of Li ring sub-networks around the GB region of $\Sigma5[001]/(120)$ tilt GB. Li-Li edge connections at the GB region are formed at different distance cutoffs ($d_{c,Li-Li}$) between 3 and 8 Å. The GB region is highlighted by a dash-line box and has a thickness of 10 Å in the GB-normal (horizontal) direction. The $d_{c,Li-Li}$ parameter can be related to the filtration level for the ring birth (b) operation in Li-ring persistence diagrams (i.e., $b = 0.5d_{c,Li-Li}$). The Li ion coordinates are taken from a 300-K MD snapshot.

References

(S1) Bollmann, W. In *Crystal Defects and Crystalline Interfaces*; Bollmann, W., Ed.; Springer: Berlin, Heidelberg, 1970; pp 143–185.

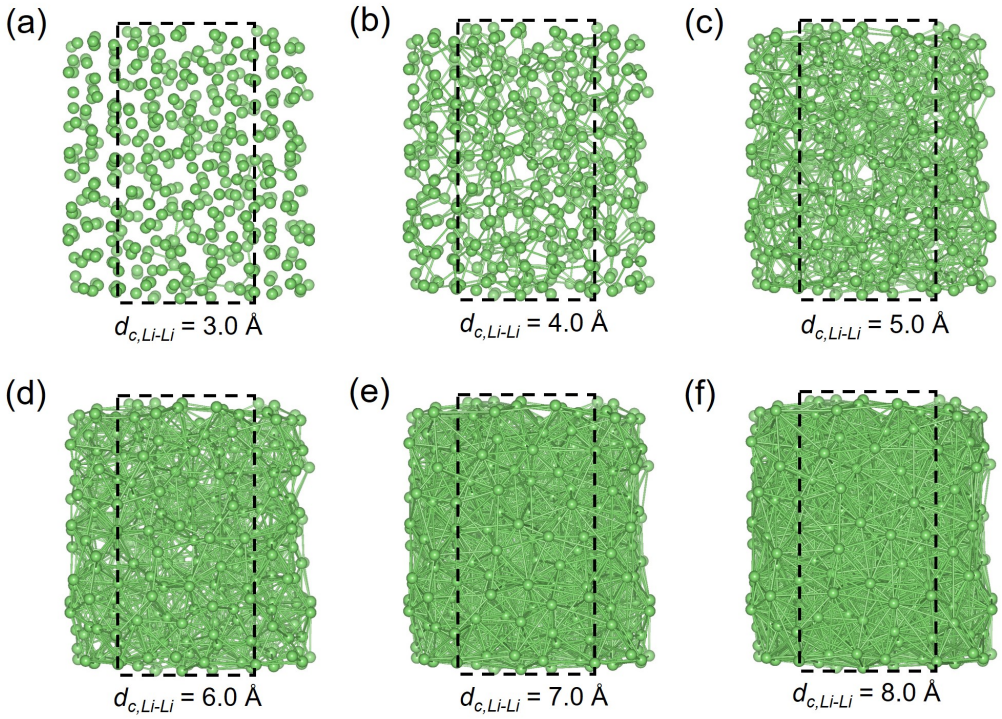

Figure S11: (a-f) Visualization of the formation of Li ring sub-networks around the GB region of $\Sigma5[001]/(001)$ twist GB. Li-Li edge connections at the GB region are formed at different distance cutoffs ($d_{c,Li-Li}$) between 3 and 8 Å. The GB region is highlighted by a dash-line box and has a thickness of 10 Å in the GB-normal (horizontal) direction. The $d_{c,Li-Li}$ parameter can be related to the filtration level for the ring birth (b) operation in Li-ring persistence diagrams (i.e., $b = 0.5d_{c,Li-Li}$). The Li ion coordinates are taken from a 300-K MD snapshot.